

Measurement of Polarization and Search for CP Violation in $B_s^0 \rightarrow \phi\phi$ Decays

T. Aaltonen,²¹ B. Álvarez González^{w,9} S. Amerio,⁴¹ D. Amidei,³² A. Anastassov,³⁶ A. Annovi,¹⁷ J. Antos,¹² G. Apollinari,¹⁵ J.A. Appel,¹⁵ A. Apresyan,⁴⁶ T. Arisawa,⁵⁶ A. Artikov,¹³ J. Asaadi,⁵¹ W. Ashmanskas,¹⁵ B. Auerbach,⁵⁹ A. Aurisano,⁵¹ F. Azfar,⁴⁰ W. Badgett,¹⁵ A. Barbaro-Galtieri,²⁶ V.E. Barnes,⁴⁶ B.A. Barnett,²³ P. Barria^{dd,44} P. Bartos,¹² M. Bauce^{bb,41} G. Bauer,³⁰ F. Bedeschi,⁴⁴ D. Beecher,²⁸ S. Behari,²³ G. Bellettini^{cc,44} J. Bellinger,⁵⁸ D. Benjamin,¹⁴ A. Beretvas,¹⁵ A. Bhatti,⁴⁸ M. Binkley^{*,15} D. Bisello^{bb,41} I. Bizjak^{hh,28} K.R. Bland,⁵ B. Blumenfeld,²³ A. Bocci,¹⁴ A. Bodek,⁴⁷ D. Bortoletto,⁴⁶ J. Boudreau,⁴⁵ A. Boveia,¹¹ L. Brigliadori^{aa,6} A. Brisuda,¹² C. Bromberg,³³ E. Brucken,²¹ M. Bucciantonio^{cc,44} J. Budagov,¹³ H.S. Budd,⁴⁷ S. Budd,²² K. Burkett,¹⁵ G. Busetto^{bb,41} P. Bussey,¹⁹ A. Buzatu,³¹ C. Calancha,²⁹ S. Camarda,⁴ M. Campanelli,²⁸ M. Campbell,³² F. Canelli^{11,15} B. Carls,²² D. Carlsmith,⁵⁸ R. Carosi,⁴⁴ S. Carrillo^{k,16} S. Carron,¹⁵ B. Casal,⁹ M. Casarsa,¹⁵ A. Castro^{aa,6} P. Catastini,²⁰ D. Cauz,⁵² V. Cavaliere,²² M. Cavalli-Sforza,⁴ A. Cerri^{e,26} L. Cerrito^{q,28} Y.C. Chen,¹ M. Chertok,⁷ G. Chiarelli,⁴⁴ G. Chlachidze,¹⁵ F. Chlebona,¹⁵ K. Cho,²⁵ D. Chokheli,¹³ J.P. Chou,²⁰ W.H. Chung,⁵⁸ Y.S. Chung,⁴⁷ C.I. Ciobanu,⁴² M.A. Ciocci^{dd,44} A. Clark,¹⁸ C. Clarke,⁵⁷ G. Compostella^{bb,41} M.E. Convery,¹⁵ J. Conway,⁷ M. Corbo,⁴² M. Cordelli,¹⁷ C.A. Cox,⁷ D.J. Cox,⁷ F. Crescioli^{cc,44} C. Cuenca Almenar,⁵⁹ J. Cuevas^{w,9} R. Culbertson,¹⁵ D. Dagenhart,¹⁵ N. d'Ascenzo^{u,42} M. Datta,¹⁵ P. de Barbaro,⁴⁷ S. De Cecco,⁴⁹ G. De Lorenzo,⁴ M. Dell'Orso^{cc,44} C. Deluca,⁴ L. Demortier,⁴⁸ J. Deng^{b,14} M. Deninno,⁶ F. Devoto,²¹ M. d'Errico^{bb,41} A. Di Canto^{cc,44} B. Di Ruzza,⁴⁴ J.R. Dittmann,⁵ M. D'Onofrio,²⁷ S. Donati^{cc,44} P. Dong,¹⁵ M. Dorigo,⁵² T. Dorigo,⁴¹ K. Ebina,⁵⁶ A. Elagin,⁵¹ A. Eppig,³² R. Erbacher,⁷ D. Errede,²² S. Errede,²² N. Ershaidat^{z,42} R. Eusebi,⁵¹ H.C. Fang,²⁶ S. Farrington,⁴⁰ M. Feindt,²⁴ J.P. Fernandez,²⁹ C. Ferrazza^{ee,44} R. Field,¹⁶ G. Flanagan^{s,46} R. Forrest,⁷ M.J. Frank,⁵ M. Franklin,²⁰ J.C. Freeman,¹⁵ Y. Funakoshi,⁵⁶ I. Furic,¹⁶ M. Gallinaro,⁴⁸ J. Galyardt,¹⁰ J.E. Garcia,¹⁸ A.F. Garfinkel,⁴⁶ P. Garosi^{dd,44} H. Gerberich,²² E. Gerchtein,¹⁵ S. Giagu^{ff,49} V. Giakoumopoulou,³ P. Giannetti,⁴⁴ K. Gibson,⁴⁵ C.M. Ginsburg,¹⁵ N. Giokaris,³ P. Giromini,¹⁷ M. Giunta,⁴⁴ G. Giurgiu,²³ V. Glagolev,¹³ D. Glenzinski,¹⁵ M. Gold,³⁵ D. Goldin,⁵¹ N. Goldschmidt,¹⁶ A. Golossanov,¹⁵ G. Gomez,⁹ G. Gomez-Ceballos,³⁰ M. Goncharov,³⁰ O. González,²⁹ I. Gorelov,³⁵ A.T. Goshaw,¹⁴ K. Goulianos,⁴⁸ S. Grinstein,⁴ C. Grosso-Pilcher,¹¹ R.C. Group^{55,15} J. Guimaraes da Costa,²⁰ Z. Gunay-Unalan,³³ C. Haber,²⁶ S.R. Hahn,¹⁵ E. Halkiadakis,⁵⁰ A. Hamaguchi,³⁹ J.Y. Han,⁴⁷ F. Happacher,¹⁷ K. Hara,⁵³ D. Hare,⁵⁰ M. Hare,⁵⁴ R.F. Harr,⁵⁷ K. Hatakeyama,⁵ C. Hays,⁴⁰ M. Heck,²⁴ J. Heinrich,⁴³ M. Herndon,⁵⁸ S. Hewamanage,⁵ D. Hidas,⁵⁰ A. Hocker,¹⁵ W. Hopkins^{f,15} D. Horn,²⁴ S. Hou,¹ R.E. Hughes,³⁷ M. Hurwitz,¹¹ U. Husemann,⁵⁹ N. Hussain,³¹ M. Hussein,³³ J. Huston,³³ G. Introzzi,⁴⁴ M. Iori^{ff,49} A. Ivanov^{o,7} E. James,¹⁵ D. Jang,¹⁰ B. Jayatilaka,¹⁴ E.J. Jeon,²⁵ M.K. Jha,⁶ S. Jindariani,¹⁵ W. Johnson,⁷ M. Jones,⁴⁶ K.K. Joo,²⁵ S.Y. Jun,¹⁰ T.R. Junk,¹⁵ T. Kamon,⁵¹ P.E. Karchin,⁵⁷ A. Kasmi,⁵ Y. Kato^{n,39} W. Ketchum,¹¹ J. Keung,⁴³ V. Khotilovich,⁵¹ B. Kilminster,¹⁵ D.H. Kim,²⁵ H.S. Kim,²⁵ H.W. Kim,²⁵ J.E. Kim,²⁵ M.J. Kim,¹⁷ S.B. Kim,²⁵ S.H. Kim,⁵³ Y.K. Kim,¹¹ N. Kimura,⁵⁶ M. Kirby,¹⁵ S. Klimenko,¹⁶ K. Kondo^{*,56} D.J. Kong,²⁵ J. Konigsberg,¹⁶ A.V. Kotwal,¹⁴ M. Kreps,²⁴ J. Kroll,⁴³ D. Krop,¹¹ N. Krumnack^{l,5} M. Kruse,¹⁴ V. Krutelyov^{c,51} T. Kuhr,²⁴ M. Kurata,⁵³ S. Kwang,¹¹ A.T. Laasanen,⁴⁶ S. Lami,⁴⁴ S. Lammel,¹⁵ M. Lancaster,²⁸ R.L. Lander,⁷ K. Lannon^{v,37} A. Lath,⁵⁰ G. Latino^{cc,44} T. LeCompte,² E. Lee,⁵¹ H.S. Lee,¹¹ J.S. Lee,²⁵ S.W. Lee^{x,51} S. Leo^{cc,44} S. Leone,⁴⁴ J.D. Lewis,¹⁵ A. Limosani^{r,14} C.-J. Lin,²⁶ J. Linacre,⁴⁰ M. Lindgren,¹⁵ E. Lipeles,⁴³ A. Lister,¹⁸ D.O. Litvintsev,¹⁵ C. Liu,⁴⁵ Q. Liu,⁴⁶ T. Liu,¹⁵ S. Lockwitz,⁵⁹ A. Loginov,⁵⁹ D. Lucchesi^{bb,41} J. Lueck,²⁴ P. Lujan,²⁶ P. Lukens,¹⁵ G. Lungu,⁴⁸ J. Lys,²⁶ R. Lysak,¹² R. Madrak,¹⁵ K. Maeshima,¹⁵ K. Makhoul,³⁰ S. Malik,⁴⁸ G. Manca^{a,27} A. Manousakis-Katsikakis,³ F. Margaroli,⁴⁶ C. Marino,²⁴ M. Martínez,⁴ R. Martínez-Ballarín,²⁹ P. Mastrandrea,⁴⁹ M.E. Mattson,⁵⁷ P. Mazzanti,⁶ K.S. McFarland,⁴⁷ P. McIntyre,⁵¹ R. McNulty^{i,27} A. Mehta,²⁷ P. Mehtala,²¹ A. Menzione,⁴⁴ C. Mesropian,⁴⁸ T. Miao,¹⁵ D. Mietlicki,³² A. Mitra,¹ H. Miyake,⁵³ S. Moed,²⁰ N. Moggi,⁶ M.N. Mondragon^{k,15} C.S. Moon,²⁵ R. Moore,¹⁵ M.J. Morello,¹⁵ J. Morlock,²⁴ P. Movilla Fernandez,¹⁵ A. Mukherjee,¹⁵ Th. Muller,²⁴ P. Murat,¹⁵ M. Mussini^{aa,6} J. Nachtman^{m,15} Y. Nagai,⁵³ J. Naganoma,⁵⁶ I. Nakano,³⁸ A. Napier,⁵⁴ J. Nett,⁵¹ C. Neu,⁵⁵ M.S. Neubauer,²² J. Nielsen^{d,26} L. Nodulman,² O. Norniella,²² E. Nurse,²⁸ L. Oakes,⁴⁰ S.H. Oh,¹⁴ Y.D. Oh,²⁵ I. Oksuzian,⁵⁵ T. Okusawa,³⁹ R. Orava,²¹ L. Ortolan,⁴ S. Pagan Griso^{bb,41} C. Pagliarone,⁵² E. Palencia^{e,9} V. Papadimitriou,¹⁵ A.A. Paramonov,² J. Patrick,¹⁵ G. Pauletta^{gg,52} M. Paulini,¹⁰ C. Paus,³⁰ D.E. Pellett,⁷ A. Penzo,⁵² T.J. Phillips,¹⁴ G. Piacentino,⁴⁴ E. Pianori,⁴³ J. Pilot,³⁷ K. Pitts,²² C. Plager,⁸ L. Pondrom,⁵⁸ K. Potamianos,⁴⁶ O. Poukhov^{*,13} F. Prokoshin^{y,13}

A. Pronko,¹⁵ F. Ptohos^g,¹⁷ E. Pueschel,¹⁰ G. Punzi^{cc},⁴⁴ J. Pursley,⁵⁸ A. Rahaman,⁴⁵ V. Ramakrishnan,⁵⁸ N. Ranjan,⁴⁶ I. Redondo,²⁹ P. Renton,⁴⁰ M. Rescigno,⁴⁹ T. Riddick,²⁸ F. Rimondi^{aa},⁶ L. Ristori⁴⁴,¹⁵ A. Robson,¹⁹ T. Rodrigo,⁹ T. Rodriguez,⁴³ E. Rogers,²² S. Rolli^h,⁵⁴ R. Roser,¹⁵ J. L. Rosner,¹¹ M. Rossi,⁵² F. Rubbo,¹⁵ F. Ruffini^{dd},⁴⁴ A. Ruiz,⁹ J. Russ,¹⁰ V. Rusu,¹⁵ A. Safonov,⁵¹ W.K. Sakumoto,⁴⁷ Y. Sakurai,⁵⁶ L. Santi^{gg},⁵² L. Sartori,⁴⁴ K. Sato,⁵³ V. Saveliev^u,⁴² A. Savoy-Navarro,⁴² P. Schlabach,¹⁵ A. Schmidt,²⁴ E.E. Schmidt,¹⁵ M.P. Schmidt*,⁵⁹ M. Schmitt,³⁶ T. Schwarz,⁷ L. Scodellaro,⁹ A. Scribano^{dd},⁴⁴ F. Scuri,⁴⁴ A. Sedov,⁴⁶ S. Seidel,³⁵ Y. Seiya,³⁹ A. Semenov,¹³ F. Sforza^{cc},⁴⁴ A. Sfyrla,²² S.Z. Shalhout,⁷ T. Shears,²⁷ P.F. Shepard,⁴⁵ M. Shimojima^t,⁵³ S. Shiraishi,¹¹ M. Shochet,¹¹ I. Shreyber,³⁴ A. Simonenko,¹³ P. Sinervo,³¹ A. Sissakian*,¹³ K. Sliwa,⁵⁴ J.R. Smith,⁷ F.D. Snider,¹⁵ A. Soha,¹⁵ S. Somalwar,⁵⁰ V. Sorin,⁴ P. Squillacioti,⁴⁴ M. Stancari,¹⁵ M. Stanitzki,⁵⁹ R. St. Denis,¹⁹ B. Stelzer,³¹ O. Stelzer-Chilton,³¹ D. Stentz,³⁶ J. Strologas,³⁵ G.L. Strycker,³² Y. Sudo,⁵³ A. Sukhanov,¹⁶ I. Suslov,¹³ K. Takemasa,⁵³ Y. Takeuchi,⁵³ J. Tang,¹¹ M. Tecchio,³² P.K. Teng,¹ J. Thom^f,¹⁵ J. Thome,¹⁰ G.A. Thompson,²² E. Thomson,⁴³ P. Ttito-Guzmán,²⁹ S. Tkaczyk,¹⁵ D. Toback,⁵¹ S. Tokar,¹² K. Tollefson,³³ T. Tomura,⁵³ D. Tonelli,¹⁵ S. Torre,¹⁷ D. Torretta,¹⁵ P. Totaro,⁴¹ M. Trovato^{ee},⁴⁴ Y. Tu,⁴³ F. Ukegawa,⁵³ S. Uozumi,²⁵ A. Varganov,³² F. Vázquez^k,¹⁶ G. Velev,¹⁵ C. Vellidis,³ M. Vidal,²⁹ I. Vila,⁹ R. Vilar,⁹ J. Vizán,⁹ M. Vogel,³⁵ G. Volpi^{cc},⁴⁴ P. Wagner,⁴³ R.L. Wagner,¹⁵ T. Wakisaka,³⁹ R. Wallny,⁸ S.M. Wang,¹ A. Warburton,³¹ D. Waters,²⁸ M. Weinberger,⁵¹ W.C. Wester III,¹⁵ B. Whitehouse,⁵⁴ D. Whiteson^b,⁴³ A.B. Wicklund,² E. Wicklund,¹⁵ S. Wilbur,¹¹ F. Wick,²⁴ H.H. Williams,⁴³ J.S. Wilson,³⁷ P. Wilson,¹⁵ B.L. Winer,³⁷ P. Wittich^g,¹⁵ S. Wolbers,¹⁵ H. Wolfe,³⁷ T. Wright,³² X. Wu,¹⁸ Z. Wu,⁵ K. Yamamoto,³⁹ J. Yamaoka,¹⁴ T. Yang,¹⁵ U.K. Yang^p,¹¹ Y.C. Yang,²⁵ W.-M. Yao,²⁶ G.P. Yeh,¹⁵ K. Yi^m,¹⁵ J. Yoh,¹⁵ K. Yorita,⁵⁶ T. Yoshida^j,³⁹ G.B. Yu,¹⁴ I. Yu,²⁵ S.S. Yu,¹⁵ J.C. Yun,¹⁵ A. Zanetti,⁵² Y. Zeng,¹⁴ and S. Zucchelli^{aa6}

(CDF Collaboration[†])

¹*Institute of Physics, Academia Sinica, Taipei, Taiwan 11529, Republic of China*

²*Argonne National Laboratory, Argonne, Illinois 60439, USA*

³*University of Athens, 157 71 Athens, Greece*

⁴*Institut de Física d'Altes Energies, ICREA, Universitat Autònoma de Barcelona, E-08193, Bellaterra (Barcelona), Spain*

⁵*Baylor University, Waco, Texas 76798, USA*

⁶*Istituto Nazionale di Fisica Nucleare Bologna, ^{aa}University of Bologna, I-40127 Bologna, Italy*

⁷*University of California, Davis, Davis, California 95616, USA*

⁸*University of California, Los Angeles, Los Angeles, California 90024, USA*

⁹*Instituto de Física de Cantabria, CSIC-University of Cantabria, 39005 Santander, Spain*

¹⁰*Carnegie Mellon University, Pittsburgh, Pennsylvania 15213, USA*

¹¹*Enrico Fermi Institute, University of Chicago, Chicago, Illinois 60637, USA*

¹²*Comenius University, 842 48 Bratislava, Slovakia; Institute of Experimental Physics, 040 01 Kosice, Slovakia*

¹³*Joint Institute for Nuclear Research, RU-141980 Dubna, Russia*

¹⁴*Duke University, Durham, North Carolina 27708, USA*

¹⁵*Fermi National Accelerator Laboratory, Batavia, Illinois 60510, USA*

¹⁶*University of Florida, Gainesville, Florida 32611, USA*

¹⁷*Laboratori Nazionali di Frascati, Istituto Nazionale di Fisica Nucleare, I-00044 Frascati, Italy*

¹⁸*University of Geneva, CH-1211 Geneva 4, Switzerland*

¹⁹*Glasgow University, Glasgow G12 8QQ, United Kingdom*

²⁰*Harvard University, Cambridge, Massachusetts 02138, USA*

²¹*Division of High Energy Physics, Department of Physics, University of Helsinki and Helsinki Institute of Physics, FIN-00014, Helsinki, Finland*

²²*University of Illinois, Urbana, Illinois 61801, USA*

²³*The Johns Hopkins University, Baltimore, Maryland 21218, USA*

²⁴*Institut für Experimentelle Kernphysik, Karlsruhe Institute of Technology, D-76131 Karlsruhe, Germany*

²⁵*Center for High Energy Physics: Kyungpook National University,*

Daegu 702-701, Korea; Seoul National University, Seoul 151-742,

Korea; Sungkyunkwan University, Suwon 440-746,

Korea; Korea Institute of Science and Technology Information,

Daejeon 305-806, Korea; Chonnam National University, Gwangju 500-757,

Korea; Chonbuk National University, Jeonju 561-756, Korea

²⁶*Ernest Orlando Lawrence Berkeley National Laboratory, Berkeley, California 94720, USA*

²⁷*University of Liverpool, Liverpool L69 7ZE, United Kingdom*

²⁸*University College London, London WC1E 6BT, United Kingdom*

²⁹*Centro de Investigaciones Energeticas Medioambientales y Tecnológicas, E-28040 Madrid, Spain*

³⁰*Massachusetts Institute of Technology, Cambridge, Massachusetts 02139, USA*

- ³¹*Institute of Particle Physics: McGill University, Montréal, Québec, Canada H3A 2T8; Simon Fraser University, Burnaby, British Columbia, Canada V5A 1S6; University of Toronto, Toronto, Ontario, Canada M5S 1A7; and TRIUMF, Vancouver, British Columbia, Canada V6T 2A3*
- ³²*University of Michigan, Ann Arbor, Michigan 48109, USA*
- ³³*Michigan State University, East Lansing, Michigan 48824, USA*
- ³⁴*Institution for Theoretical and Experimental Physics, ITEP, Moscow 117259, Russia*
- ³⁵*University of New Mexico, Albuquerque, New Mexico 87131, USA*
- ³⁶*Northwestern University, Evanston, Illinois 60208, USA*
- ³⁷*The Ohio State University, Columbus, Ohio 43210, USA*
- ³⁸*Okayama University, Okayama 700-8530, Japan*
- ³⁹*Osaka City University, Osaka 588, Japan*
- ⁴⁰*University of Oxford, Oxford OX1 3RH, United Kingdom*
- ⁴¹*Istituto Nazionale di Fisica Nucleare, Sezione di Padova-Trento, ^{bb}University of Padova, I-35131 Padova, Italy*
- ⁴²*LPNHE, Université Pierre et Marie Curie/IN2P3-CNRS, UMR7585, Paris, F-75252 France*
- ⁴³*University of Pennsylvania, Philadelphia, Pennsylvania 19104, USA*
- ⁴⁴*Istituto Nazionale di Fisica Nucleare Pisa, ^{cc}University of Pisa, ^{dd}University of Siena and ^{ee}Scuola Normale Superiore, I-56127 Pisa, Italy*
- ⁴⁵*University of Pittsburgh, Pittsburgh, Pennsylvania 15260, USA*
- ⁴⁶*Purdue University, West Lafayette, Indiana 47907, USA*
- ⁴⁷*University of Rochester, Rochester, New York 14627, USA*
- ⁴⁸*The Rockefeller University, New York, New York 10065, USA*
- ⁴⁹*Istituto Nazionale di Fisica Nucleare, Sezione di Roma 1, ^{ff}Sapienza Università di Roma, I-00185 Roma, Italy*
- ⁵⁰*Rutgers University, Piscataway, New Jersey 08855, USA*
- ⁵¹*Texas A&M University, College Station, Texas 77843, USA*
- ⁵²*Istituto Nazionale di Fisica Nucleare Trieste/Udine, I-34100 Trieste, ^{gg}University of Udine, I-33100 Udine, Italy*
- ⁵³*University of Tsukuba, Tsukuba, Ibaraki 305, Japan*
- ⁵⁴*Tufts University, Medford, Massachusetts 02155, USA*
- ⁵⁵*University of Virginia, Charlottesville, Virginia 22906, USA*
- ⁵⁶*Waseda University, Tokyo 169, Japan*
- ⁵⁷*Wayne State University, Detroit, Michigan 48201, USA*
- ⁵⁸*University of Wisconsin, Madison, Wisconsin 53706, USA*
- ⁵⁹*Yale University, New Haven, Connecticut 06520, USA*
- (Dated: January 13, 2014)

We present the first measurement of polarization and CP -violating asymmetries in a B_s^0 decay into two light vector mesons, $B_s^0 \rightarrow \phi\phi$, and an improved determination of its branching ratio using 295 decays reconstructed in a data sample corresponding to 2.9 fb^{-1} of integrated luminosity collected by the CDF experiment at the Fermilab Tevatron collider. The fraction of longitudinal polarization is determined to be $f_L = 0.348 \pm 0.041(\text{stat}) \pm 0.021(\text{syst})$, and the branching ratio $\mathcal{B}(B_s^0 \rightarrow \phi\phi) = [2.32 \pm 0.18(\text{stat}) \pm 0.82(\text{syst})] \times 10^{-5}$. Asymmetries of decay angle distributions sensitive to CP violation are measured to be $A_u = -0.007 \pm 0.064(\text{stat}) \pm 0.018(\text{syst})$ and $A_v = -0.120 \pm 0.064(\text{stat}) \pm 0.016(\text{syst})$.

PACS numbers: 13.25.Hw 11.30.Er 14.40.Nd 12.38.Qk

*Deceased

[†]With visitors from ^aIstituto Nazionale di Fisica Nucleare, Sezione di Cagliari, 09042 Monserrato (Cagliari), Italy, ^bUniversity of CA Irvine, Irvine, CA 92697, USA, ^cUniversity of CA Santa Barbara, Santa Barbara, CA 93106, USA, ^dUniversity of CA Santa Cruz, Santa Cruz, CA 95064, USA, ^eCERN, CH-1211 Geneva, Switzerland, ^fCornell University, Ithaca, NY 14853, USA, ^gUniversity of Cyprus, Nicosia CY-1678, Cyprus, ^hOffice of Science, U.S. Department of Energy, Washington, DC 20585, USA, ⁱUniversity College Dublin, Dublin 4, Ireland, ^jUniversity of Fukui, Fukui City, Fukui Prefecture, Japan 910-0017, ^kUniversidad Iberoamericana, Mexico D.F., Mexico, ^lIowa State University, Ames, IA 50011, USA, ^mUniversity of Iowa, Iowa City, IA 52242, USA, ⁿKinki University,

Higashi-Osaka City, Japan 577-8502, ^oKansas State University, Manhattan, KS 66506, USA, ^pUniversity of Manchester, Manchester M13 9PL, United Kingdom, ^qQueen Mary, University of London, London, E1 4NS, United Kingdom, ^rUniversity of Melbourne, Victoria 3010, Australia, ^sMuons, Inc., Batavia, IL 60510, USA, ^tNagasaki Institute of Applied Science, Nagasaki, Japan, ^uNational Research Nuclear University, Moscow, Russia, ^vUniversity of Notre Dame, Notre Dame, IN 46556, USA, ^wUniversidad de Oviedo, E-33007 Oviedo, Spain, ^xTexas Tech University, Lubbock, TX 79609, USA, ^yUniversidad Tecnica Federico Santa Maria, 110v Valparaiso, Chile, ^zYarmouk University, Irbid 211-63, Jordan, ^{hh}On leave from J. Stefan Institute, Ljubljana, Slovenia,

Several charmless B_s^0 decays were observed at the Tevatron in Run II [1, 2], but a detailed investigation of decay properties and of CP violation in these decays is still lacking. The $B_s^0 \rightarrow \phi\phi$ process is mediated by a one-loop flavor-changing neutral current, the $b \rightarrow s$ penguin, and belongs to the class of decays where the final state consists of a pair of light spin-1 mesons (V). Three independent amplitudes govern $B \rightarrow VV$ decays, corresponding to the polarizations of the final-state vector mesons: longitudinal polarization, and transverse polarization with spins parallel or perpendicular to each other. The first two states are CP -even, while the last one is CP -odd. Polarization amplitudes can be measured analyzing angular distributions of final-state particles. Interference between the CP -even and CP -odd amplitudes can generate asymmetries in angular distributions, the triple product (TP) asymmetries, which may signal unexpected CP violation due to physics beyond the standard model (SM).

The V-A structure of charged weak currents leads to the expectation of a dominant longitudinal polarization [3, 4]. Approximately equal longitudinal and transverse polarizations have been measured instead in $b \rightarrow s$ penguin-dominated B^0 and B^+ decay modes [5]. This is explained in the SM by including either non-factorizable penguin-annihilation effects [6] or final state interactions [7]. Recent theoretical predictions [3, 4] indicate a longitudinal fraction f_L in the 40–70 % range, when phenomenological parameters are adjusted to accommodate present experimental data. Explanations involving new physics (NP) in the $b \rightarrow s$ penguin process have also been proposed [8]. Additional experimental information in B_s^0 penguin-dominated decays, such as $B_s^0 \rightarrow \phi\phi$, may help distinguishing the various solutions [9], and can be used to derive upper limits for the mixing-induced CP asymmetries [10].

Triple product asymmetries are odd under time-reversal (T), and can be generated either by final-state interactions or CP violation. In flavor-untagged samples, where the initial B flavor is not identified, TP asymmetries can be shown to signify genuine CP violation [11]. In this respect they are very sensitive to the presence of NP in the decay since they do not require a strong-phase difference between NP and SM amplitudes, as opposed to direct CP asymmetries [12]. The TP asymmetry is defined as $\mathcal{A}_{TP} = \frac{\Gamma(\text{TP}>0) - \Gamma(\text{TP}<0)}{\Gamma(\text{TP}>0) + \Gamma(\text{TP}<0)}$, where Γ is the decay width for the given process. In $B_s^0 \rightarrow \phi\phi$ decays two TP asymmetries can be studied, corresponding to the two interference terms between amplitudes with different CP . These asymmetries are predicted to vanish in the SM, and an observation of a non-zero asymmetry would be an unambiguous sign of NP [12].

In this Letter we present the first measurement of polarization amplitudes and of TP asymmetries in the $B_s^0 \rightarrow \phi\phi$ decay and an updated measurement of its

branching ratio using $B_s^0 \rightarrow J/\psi\phi$ decays reconstructed in the same dataset as a normalization. Data from an integrated luminosity of 2.9 fb^{-1} of $p\bar{p}$ collisions at $\sqrt{s} = 1.96 \text{ TeV}$ are analyzed.

The components of the CDF II detector relevant for this analysis are briefly described below; a more complete description can be found elsewhere [13]. We reconstruct charged-particle trajectories (tracks) in the pseudorapidity range $|\eta| \lesssim 1$ [14] using a silicon microstrip vertex detector [15] and a central drift chamber [16], both immersed in a 1.4 T solenoidal magnetic field. The detection of muons in the pseudorapidity range $|\eta| \lesssim 0.6$ is provided by two sets of drift chambers located behind the calorimeters (CMU) and behind additional steel absorbers (CMP), while the CMX detector covers the range $0.6 \lesssim |\eta| \lesssim 1.0$ [17]. A sample enriched with heavy-flavor particles is selected by the displaced-track trigger [18], based on the Silicon Vertex Trigger (SVT) [19]. It provides a precise measurement of the track impact parameter (d_0), defined as the distance of closest approach to the beam axis in the transverse plane. Decays of heavy-flavor particles are identified by requiring two tracks with $120 \mu\text{m} \leq d_0 \leq 1.0 \text{ mm}$ and applying a requirement on the two-dimensional decay length, $L_{xy} > 200 \mu\text{m}$ [20].

We reconstruct B_s^0 mesons by first forming $\phi \rightarrow K^+ K^-$ and $J/\psi \rightarrow \mu^+ \mu^-$ candidate decays from opposite-sign track pairs with mass within 15 and 100 MeV/c^2 of the known [21] ϕ and J/ψ mass, respectively. At least one J/ψ track is required to match a segment reconstructed in the muon detectors. We form $B_s^0 \rightarrow \phi\phi$ ($B_s^0 \rightarrow J/\psi\phi$) candidates by fitting to a single vertex the $\phi\phi$ ($J/\psi\phi$) candidate pairs. In the $B_s^0 \rightarrow J/\psi\phi$ case the fit constrains the mass of the two muons to the J/ψ mass [21]. At least one pair of tracks in the B_s^0 candidate must satisfy the trigger requirements. Combinatorial background and partially reconstructed decays are reduced by exploiting the long lifetime and relatively hard p_T spectrum of B_s^0 mesons. We follow closely the selection adopted in [1], using the vertex fit χ^2 , the L_{xy} , the reconstructed B_s^0 and ϕ meson impact parameters, and the minimum kaon transverse momentum as discriminating variables. The selection requirements are set by maximizing the quantity $S/\sqrt{S+B}$, where the accepted number of signal events S is derived from a Monte Carlo (MC) simulation [22] of the CDF II detector and trigger, while the number of background events B is modeled using data in mass sideband regions: (5.02, 5.22) and (5.52, 5.72) GeV/c^2 . The resulting mass distributions are shown in Fig. 1.

A binned maximum likelihood (ML) fit to the m_B distribution is performed to determine the B_s^0 yield for both decay modes. The signal is parameterized by two Gaussian functions with the same mean value, but different widths. The ratios between the two widths and between the integrals of the two components are fixed based on MC simulations. The combinatorial background has a smooth mass distribution near the signal

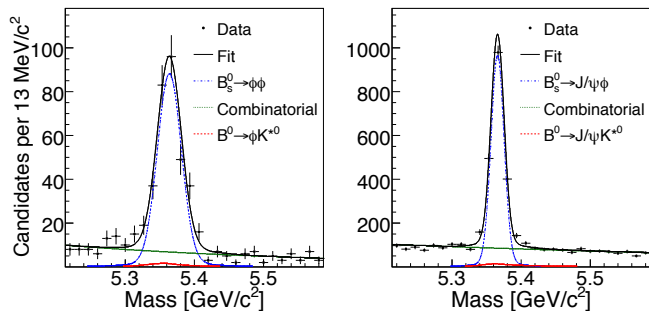


FIG. 1: The invariant mass of the four kaons (left) and of the J/ψ and two kaons (right) for $B_s^0 \rightarrow \phi\phi$ and $B_s^0 \rightarrow J/\psi\phi$ candidates, overlaid with fit projections and separate signal and background components. The narrower signal peak for the $B_s^0 \rightarrow J/\psi\phi$ is due to the J/ψ mass constraint applied in the reconstruction.

and is modeled with an exponential function. A reflection from $B^0 \rightarrow \phi K^*(892)^0$ ($B^0 \rightarrow J/\psi K^*(892)^0$) with misassigned kaon mass to final state pions contaminates the $B_s^0 \rightarrow \phi\phi$ ($B_s^0 \rightarrow J/\psi\phi$) signal region. Parameterizations and efficiencies determined from simulation are used for these backgrounds. Their normalizations are derived from the known [21] branching ratios, fragmentation fraction ratio f_s/f_d , and the ratio of the detection efficiencies relative to signal ones. We estimate $(4.19 \pm 0.93)\%$ and $(2.7 \pm 1.0)\%$ reflection background under the $B_s^0 \rightarrow J/\psi\phi$ and $B_s^0 \rightarrow \phi\phi$ signals, respectively. Free parameters of the fit are the signal fraction, the B_s^0 mass M , and width σ , together with the exponential slope b_0 defining the combinatorial background mass shape. We estimate the total number of signal decays as $N_{\phi\phi} = 295 \pm 20(\text{stat}) \pm 12(\text{syst})$ and $N_{\psi\phi} = 1766 \pm 48(\text{stat}) \pm 41(\text{syst})$, where the systematic uncertainty is estimated by varying signal and background models.

The $B_s^0 \rightarrow \phi\phi$ decay rate is derived from the relation

$$\frac{\mathcal{B}(B_s^0 \rightarrow \phi\phi)}{\mathcal{B}(B_s^0 \rightarrow J/\psi\phi)} = \frac{N_{\phi\phi}}{N_{\psi\phi}} \frac{\mathcal{B}(J/\psi \rightarrow \mu\mu)}{\mathcal{B}(\phi \rightarrow KK)} \frac{\epsilon_{\psi\phi}}{\epsilon_{\phi\phi}} \epsilon_{\psi\phi}^{\mu} \epsilon_{\phi\phi}^{\mu},$$

where $\epsilon_{\psi\phi}/\epsilon_{\phi\phi}$ is the acceptance times efficiency ratio for the two decays and $\epsilon_{\psi\phi}^{\mu}$ is the efficiency for identifying at least one of the two muons. The efficiency ratio is determined using a MC simulation of the CDF II detector and trigger, whose reliability in determining relative trigger and reconstruction efficiencies has been verified for several different decay modes also using data-driven approaches [23]. We estimate $\epsilon_{\psi\phi}/\epsilon_{\phi\phi} = 0.939 \pm 0.099$, where the uncertainty includes systematic effects from polarization uncertainties in the two decay modes (9%), from the different trigger efficiencies for kaons and muons (4%), and from the B_s^0 p_T spectra (1%). We use inclusive J/ψ data to derive the single-muon identification efficiency as a function of muon p_T . It is determined separately in two pseudorapidity regions corre-

sponding, respectively, to the CMU/CMP and CMX detectors, and is described by a turn-on function that depends on a plateau, a slope, and a threshold parameter. We use simulated $B_s^0 \rightarrow J/\psi\phi$ decays to calculate $\epsilon_{\psi\phi}^{\mu}$ treating the efficiencies for the two muons as uncorrelated: $\epsilon_{\psi\phi}^{\mu} = (86.95 \pm 0.44(\text{stat}) \pm 0.75(\text{syst}))\%$. The systematic uncertainty includes the uncertainty on the background subtraction and effects of residual correlation between the two muon efficiencies.

We measure $\mathcal{B}(B_s^0 \rightarrow \phi\phi)/\mathcal{B}(B_s^0 \rightarrow J/\psi\phi) = [1.78 \pm 0.14(\text{stat}) \pm 0.20(\text{syst})] \times 10^{-2}$ and derive $\mathcal{B}(B_s^0 \rightarrow \phi\phi) = [2.32 \pm 0.18(\text{stat}) \pm 0.26(\text{syst}) \pm 0.78(\text{br})] \times 10^{-5}$, using the known [21] $\mathcal{B}(B_s^0 \rightarrow J/\psi\phi)$, which contributes the dominant uncertainty, labeled (br). This result is in agreement and supersedes our previous measurement [1] with a substantial reduction of its statistical uncertainty; it is also consistent with recent theoretical calculations [3, 4].

We describe the angular distribution of the $B_s^0 \rightarrow \phi\phi$ decay products using the helicity variables $\vec{\omega} = (\cos\vartheta_1, \cos\vartheta_2, \Phi)$, where ϑ_i is the angle between the direction of the K^+ from each ϕ and the direction opposite the B_s^0 in the vector meson rest frame, and Φ is the angle between the two resonance decay planes in the B_s^0 rest frame. The three independent complex amplitudes are A_0 for the longitudinal polarization and A_{\parallel} (A_{\perp}) for transverse polarization with spins parallel (perpendicular) to each other. They are related by $|A_0|^2 + |A_{\parallel}|^2 + |A_{\perp}|^2 = 1$. The differential decay rate is expressed as $d^4\Gamma/(dtd\vec{\omega}) \propto \sum_{i=1}^6 K_i(t) f_i(\vec{\omega})$, where the functions $K_i(t)$ encode the B_s^0 time evolution including mixing and depend on the polarization amplitudes, and the $f_i(\vec{\omega})$ are functions of the helicity angles only [12]. To extract the polarization amplitudes we measure the time-integrated angular distribution assuming no direct CP violation and a negligible weak phase difference between B_s^0 mixing and $B_s^0 \rightarrow \phi\phi$ decay as predicted in the SM. The time-integrated differential decay rate depends on the polarization amplitudes at $t = 0$ and on the light and heavy B_s^0 mass-eigenstate lifetimes, τ_L and τ_H , as follows:

$$\begin{aligned} \frac{d^3\Gamma}{d\vec{\omega}} &\propto \tau_L (|A_0|^2 f_1(\vec{\omega}) + |A_{\parallel}|^2 f_2(\vec{\omega}) \\ &\quad + |A_0||A_{\parallel}| \cos\delta_{\parallel} f_5(\vec{\omega})) + \tau_H |A_{\perp}|^2 f_3(\vec{\omega}), \end{aligned} \quad (1)$$

where $\delta_{\parallel} = \arg(A_0^* A_{\parallel})$ and

$$\begin{aligned} f_1(\vec{\omega}) &= 4 \cos^2\vartheta_1 \cos^2\vartheta_2, \\ f_2(\vec{\omega}) &= \sin^2\vartheta_1 \sin^2\vartheta_2 (1 + \cos 2\Phi), \\ f_3(\vec{\omega}) &= \sin^2\vartheta_1 \sin^2\vartheta_2 (1 - \cos 2\Phi), \\ f_5(\vec{\omega}) &= \sqrt{2} \sin 2\vartheta_1 \sin 2\vartheta_2 \cos\Phi. \end{aligned}$$

Two triple products are present in $B \rightarrow VV$ decays: $\text{TP}_2 \equiv \Im(A_{\parallel}^* A_{\perp})$, and $\text{TP}_1 \equiv \Im(A_0^* A_{\perp})$. These factors appear, respectively, in the decay rate terms $K_4(t)$ and

$K_6(t)$ multiplied by the functions

$$f_4(\vec{\omega}) = -2 \sin^2 \vartheta_1 \sin^2 \vartheta_2 \sin 2\Phi,$$

$$f_6(\vec{\omega}) = -\sqrt{2} \sin 2\vartheta_1 \sin 2\vartheta_2 \sin \Phi.$$

In flavor-untagged samples the TP terms, that vanish in the absence of NP, are proportional to the so-called *true* triple products, and provide two CP -violating observables, $\mathcal{A}_{\text{TP}}^1$ and $\mathcal{A}_{\text{TP}}^2$ [11]. We access $\mathcal{A}_{\text{TP}}^2$ through the observable $u = \sin 2\Phi$. We measure the u asymmetry, A_u , by integrating over $\cos \vartheta_{1,2}$ the untagged decay rate and counting events with $u > 0$ (N_u^+) and $u < 0$ (N_u^-). Similarly, $\mathcal{A}_{\text{TP}}^1$ is accessed through an asymmetry in $\sin \Phi$. We define the observable v as $v = \sin \Phi$ ($v = -\sin \Phi$) if $\cos \vartheta_1 \cos \vartheta_2 \geq 0$ ($\cos \vartheta_1 \cos \vartheta_2 < 0$) and measure its asymmetry A_v by counting events with $v > 0$ (N_v^+) and $v < 0$ (N_v^-). The asymmetries are defined as

$$A_{u(v)} = \frac{N_{u(v)}^+ - N_{u(v)}^-}{N_{u(v)}^+ + N_{u(v)}^-} = \mathcal{N}_{u(v)} \times$$

$$[\Im(A_{\parallel(0)}^* A_{\perp}) + \Im(\bar{A}_{\parallel(0)}^* \bar{A}_{\perp})] = \mathcal{N}_{u(v)} \mathcal{A}_{\text{TP}}^{2(1)}, (2)$$

where the two normalization factors are $\mathcal{N}_u = -2/\pi$ and $\mathcal{N}_v = -\sqrt{2}/\pi$. Both A_u and A_v are proportional to CP -violating TP asymmetries, and are also sensitive to mixing-induced TP when considering the decay-width difference of the B_s^0 system.

We perform an unbinned ML fit to the reconstructed mass of the B_s^0 candidates and the helicity angles in order to measure the polarization amplitudes. The contribution of each candidate to the likelihood is $\mathcal{L}_i = f_s \mathcal{P}_s(m_{B_i}, \vec{\omega}_i | \vec{\xi}_s) + (1 - f_s) \mathcal{P}_b(m_{B_i}, \vec{\omega}_i | \vec{\xi}_b)$, where f_s is the signal fraction and \mathcal{P}_j are the probability density functions (PDFs) for the $B_s^0 \rightarrow \phi\phi$ signal ($j = s$) and background ($j = b$) components, which depend on the fit parameters $\vec{\xi}_s$ and $\vec{\xi}_b$, respectively. The effects of neglecting the reflection background are included in the systematic uncertainties. Both the signal and the background PDFs are the products of a mass component, described earlier, and an angular one. The signal angular component is given by Eq. 1 multiplied by an acceptance factor. The acceptance is computed in bins of the helicity angles from simulated $B_s^0 \rightarrow \phi\phi$ decays averaged over all possible spin states of the decay products and passed through detector simulation, full reconstruction, and analysis cuts. We use an empirical parameterization derived from the observed angular distributions in the mass sidebands to model the background angular PDF: the product of a flat distribution for the Φ angle and a parabolic function for the other two, whose single parameter b_1 is a fit parameter. We fix τ_L and τ_H to the world average values [21]. There are eight free parameters in the fit: f_s , $\vec{\xi}_s = (M, \sigma, |A_0|^2, |A_{\parallel}|^2, \cos \delta_{\parallel})$ and $\vec{\xi}_b = (b_0, b_1)$. The fit has been extensively tested using

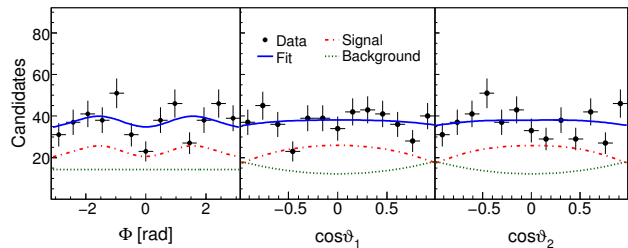


FIG. 2: Angular distribution for $B_s^0 \rightarrow \phi\phi$ events with the fit projection, signal, and background component superimposed.

simulated samples with a variety of input parameters and shows unbiased estimates of parameters and their uncertainties. We also perform the polarization measurement using the sample of ≈ 1700 $B_s^0 \rightarrow J/\psi\phi$ candidates described earlier. We find $|A_0|^2 = 0.534 \pm 0.019(\text{stat})$ and $|A_{\parallel}|^2 = 0.220 \pm 0.025(\text{stat})$, in good agreement with current measurements [24]. The results of the polarization analysis for the $B_s^0 \rightarrow \phi\phi$ sample are summarized in Table I. In Fig. 2 we show the fit projections onto the helicity angles. The dominant correlation of the fit parameters is between $|A_0|^2$ and $|A_{\parallel}|^2$ (-0.447), the others being much smaller. Several sources of systematic uncertainty

TABLE I: Summary of the $B_s^0 \rightarrow \phi\phi$ measurements. The first uncertainty quoted is statistical and the second is systematic.

Observable	Result
\mathcal{B}	$[2.32 \pm 0.18 \pm 0.82] \times 10^{-5}$
$ A_0 ^2$	$0.348 \pm 0.041 \pm 0.021$
$ A_{\parallel} ^2$	$0.287 \pm 0.043 \pm 0.011$
$ A_{\perp} ^2$	$0.365 \pm 0.044 \pm 0.027$
$\cos \delta_{\parallel}$	$-0.91^{+0.15}_{-0.13} \pm 0.09$
A_u	$-0.007 \pm 0.064 \pm 0.018$
A_v	$-0.120 \pm 0.064 \pm 0.016$

have been studied. We account for the neglected physics backgrounds considering the $B^0 \rightarrow \phi K^*(892)^0$ decay and two other possible contaminations: $B_s^0 \rightarrow \phi f_0(980)$, with $f_0 \rightarrow K^+ K^-$, and $B_s^0 \rightarrow \phi K^+ K^-$ (non-resonant). The latter two contributions are normalized to the signal yield in analogy with similar $B^0 \rightarrow \phi X$ decays. We assume up to 4.6% contamination from $B_s^0 \rightarrow \phi f_0$ and 0.9% of $B_s^0 \rightarrow \phi K^+ K^-$, and determine a 1.5%(0.4%) shift in the central value for $|A_0|^2$ ($|A_{\parallel}|^2$) using simulated experiments. Biases introduced by the time integration are examined with MC simulation: they are created by the dependence of the angular acceptance on $\Delta\Gamma_s$ and by a non-uniform acceptance in the B_s^0 proper decay time introduced by the displaced-track trigger. The assigned systematic uncertainty (1%) is the full shift expected in the central value, assuming a value for $\Delta\Gamma_s$ equal to the world average plus one standard deviation [21]. We also

consider the propagation of $\tau_{L(H)}$ uncertainties to the polarization amplitudes (1%). Other sources of minor systematic uncertainties are the modeling of the combinatorial background (0.4%) and of the angular acceptance (0.5%). The impact of CP -violating effects on the measured amplitudes is negligible.

The asymmetries A_i ($i = u, v$) are evaluated through an unbinned ML fit to m_B only, using the joint likelihood for the N_i^+ and N_i^- events with positive and negative $u(v)$. The same m_B PDF parameterization discussed above is used for samples with both $u(v)$ signs. We multiply the total likelihood by the binomial $f(N_i^+, N_i^- | p)$, where the probability p of obtaining N_i^+ and N_i^- events depends on the overall signal fraction f_s , the signal asymmetry A_i , and the background asymmetry A_b^i : $p = \frac{1}{2}[1 + A_i f_s + (1 - f_s) A_b^i]$. Mass and width for the B_s^0 signal, as well as signal fraction, are consistent with those obtained in the polarization analysis, while background asymmetries are consistent with zero. The measured $B_s^0 \rightarrow \phi\phi$ asymmetries are reported in Table I. The systematic uncertainty is evaluated using an alternate background parameterization as in the polarization analysis and by conservatively assigning maximal asymmetry to the neglected physics background peaking in the signal region. Using a large sample of simulated events, we check that the detector acceptance and resolution introduce a bias in the asymmetries smaller than 0.2%.

In summary, we measure for the first time the polarization amplitudes and the triple product asymmetries in the $B_s^0 \rightarrow \phi\phi$ decay. We find a significantly suppressed longitudinal fraction $f_L = |A_0|^2 = 0.348 \pm 0.041(\text{stat}) \pm 0.021(\text{syst})$, smaller than in other $b \rightarrow s$ penguin $B \rightarrow VV$ decays [5]. This result agrees well with predictions [3] based on QCD factorization, but only marginally with perturbative QCD ones [4], and hints at a large penguin annihilation contribution [9]. The two measured asymmetries are statistically consistent with the no CP violation hypothesis, although A_v is 1.8σ different from zero.

We thank D. London, A. Datta, M. Gronau, and I. Bigi for valuable discussions on time-integrated TP asymmetries. We thank the Fermilab staff and the technical staffs of the participating institutions for their vital contributions. This work was supported by the U.S. Department of Energy and National Science Foundation; the Italian Istituto Nazionale di Fisica Nucleare; the Ministry of Education, Culture, Sports, Science and Technology of Japan; the Natural Sciences and Engineering Research Council of Canada; the National Science Council of the Republic of China; the Swiss National Science Foundation; the A.P. Sloan Foundation; the Bundesministerium für Bildung und Forschung, Germany; the Korean World Class University Program, the National Research Foundation of Korea; the Science and Technology Facilities Council and the Royal Society, UK; the Russian Foundation for Basic Research; the Ministerio de Ciencia e Innovación, and Programa Consolider-Ingenio 2010, Spain;

the Slovak R&D Agency; the Academy of Finland; and the Australian Research Council (ARC).

-
- [1] D. Acosta *et al.* (CDF Collaboration), Phys. Rev. Lett. **95**, 031801 (2005).
 - [2] A. Abulencia *et al.* (CDF Collaboration), Phys. Rev. Lett. **97**, 211802 (2006).
 - [3] M. Beneke, J. Rohrer, and D. Yang, Nucl. Phys. **B774**, 64 (2007); H. Y. Cheng and C. K. Chua, Phys. Rev. D **80**, 114026 (2009).
 - [4] A. Ali *et al.*, Phys. Rev. D **76**, 074018 (2007).
 - [5] B. Aubert *et al.* (BABAR Collaboration), Phys. Rev. Lett. **98**, 051801 (2007), Phys. Rev. Lett. **99**, 201802 (2007); K.-F. Chen *et al.* (Belle Collaboration), Phys. Rev. Lett. **94**, 221804 (2005).
 - [6] A. L. Kagan, Phys. Lett. B **601**, 151 (2004).
 - [7] For an overview see A. Datta *et al.*, Phys. Rev. D **76**, 034015 (2007) and references therein.
 - [8] C. S. Huang *et al.*, Phys. Rev. D **73**, 034026 (2006); C. Chen and C. Geng, Phys. Rev. D **71**, 115004 (2005).
 - [9] A. Datta *et al.*, Eur. Phys. J. C **60**, 279 (2009).
 - [10] M. Bartsch, G. Buchalla, and C. Kraus, arXiv:0810.0249 [hep-ph].
 - [11] A. Datta, M. Duraisamy, and D. London, Phys. Lett. B **701**, 357 (2011); M. Gronau and J. L. Rosner, arXiv:1107.1232 [hep-ph].
 - [12] G. Valencia, Phys. Rev. D **39**, 3339 (1989); A. Datta and D. London, Int. J. Mod. Phys. A **19**, 2505 (2004).
 - [13] D. Acosta *et al.* (CDF Collaboration), Phys. Rev. D **71**, 032001 (2005).
 - [14] CDF uses a cylindrical coordinate system with the z axis along the proton beam axis. Pseudorapidity is $\eta \equiv \ln(\tan(\vartheta/2))$, where ϑ is the polar angle, and ϕ is the azimuthal angle while $p_T = |p| \sin(\vartheta)$.
 - [15] C.S. Hill, Nucl. Instrum. Methods A **530**, 1 (2004); A. Sill *et al.*, Nucl. Instrum. Methods A **447**, 1 (2000); A. Affolder *et al.*, Nucl. Instrum. Methods A **453**, 84 (2000).
 - [16] T. Affolder *et al.*, Nucl. Instrum. Methods A **526**, 249 (2004).
 - [17] G. Ascoli *et al.*, Nucl. Instrum. Methods A **268**, 33(1988).
 - [18] A. Abulencia *et al.* (CDF Collaboration), Phys. Rev. Lett. **98**, 061802 (2007).
 - [19] W. Ashmanskas *et al.*, Nucl. Instrum. Methods A **518**, 532 (2004); G. Punzi and L. Ristori, Ann. Rev. Nucl. Part. Sci. **60**, 595 (2010).
 - [20] L_{xy} is calculated as the displacement of the two-track intersection point with respect to the beam axis, projected onto the total transverse momentum of the track pair.
 - [21] K. Nakamura *et al.* (Particle Data Group), J. Phys. G **37**, 075021 (2010).
 - [22] E. Gerchtein and M. Paulini, eConf **C0303241**, TUMT005 (2003), arXiv:physics/0306031.
 - [23] D. Acosta *et al.* (CDF Collaboration), Phys. Rev. Lett. **94**, 122001 (2005); T. Aaltonen *et al.* (CDF Collaboration), Phys. Rev. Lett. **103**, 031801 (2009); A. Abulencia *et al.* (CDF Collaboration), Phys. Rev. Lett. **98**, 122002 (2007).
 - [24] T. Aaltonen *et al.* (CDF Collaboration), Phys. Rev. Lett.

100, 121803 (2008); V. M. Abazov *et al.* (D0 Collaboration), Phys. Rev. Lett. **102**, 032001 (2009).